Conformational and thermodynamic characterization of the premolten globule state occurring during unfolding of the molten globule state of cytochrome c

ARTICLE *in* EUROPEAN JOURNAL OF BIOCHEMISTRY · NOVEMBER 2010

Impact Factor: 2.54 · DOI: 10.1007/s00775-010-0691-5 · Source: PubMed

6 AUTHORS, INCLUDING:

Md Imtaiyaz Hassan
Jamia Millia Islamia
108 PUBLICATIONS **956** CITATIONS
SEE PROFILE

Tej P Singh
All India Institute of Medical Sciences
415 PUBLICATIONS **5,121** CITATIONS
SEE PROFILE

Ali A Moosavi-Movahedi
University of Tehran
520 PUBLICATIONS **5,461** CITATIONS
SEE PROFILE

Faizan Ahmad
Jamia Millia Islamia
219 PUBLICATIONS **2,536** CITATIONS
SEE PROFILE

J Biol Inorg Chem (2009) 14:751–760
DOI 10.1007/s00775-009-0488-6

ORIGINAL PAPER

A single mutation induces molten globule formation and a drastic destabilization of wild-type cytochrome *c* at pH 6.0

Md. Khurshid Alam Khan · Utpal Das · Md. Hamidur Rahaman · Md. Imtaiyaz Hassan · A. Srinivasan · Tej P. Singh · Faizan Ahmad

Received: 31 October 2008 / Accepted: 20 February 2009 / Published online: 10 March 2009

Abstract Amino acid sequences of seven subfamilies of cytochromes *c* show that other than heme binding residues there are only four positions which are conserved in all subfamilies: Gly/Ala6, Phe/Tyr10, Leu/Val/Phe94, and Tyr/Trp/Phe97. These residues are 90% conserved in all sequences reported and are also considered to be involved in a common folding nucleus. To determine the importance of conserved interactions offered by the side chain of Leu94, we made an L94G mutant of horse cytochrome *c*. Characterization of this mutant by the far-UV, near-UV, and Soret circular dichroism, intrinsic and 1-Anilino-8-naphthalene sulfonate fluorescence, and dynamic light scattering measurements led to the conclusion that the L94G mutant has all the common structural characteristics of a molten globule at pH 6.0 and 25 °C. NaCl induces a cooperative transition between the acid-denatured state and a state of L94G having all the common structural characteristics of a pre-molten-globule state at pH 2 and 25 °C. Thermal denaturation studies showed that the midpoint of denaturation of the mutant is 28 °C less than that of the wild-type protein. Interestingly, the structure analysis using the coordinates given in the Protein Data Bank (1hrc) also suggested that the L94G mutant would be less stable than the wild-type protein.

Keywords Site-directed mutagenesis · Molten globule · Pre-molten globule · Thermal stability · Cytochrome *c*

Md. Khurshid Alam Khan · Md. Hamidur Rahaman · Md. Imtaiyaz Hassan · F. Ahmad (✉)
Centre for Interdisciplinary Research in Basic Sciences,
Jamia Millia Islamia,
New Delhi 110025, India
e-mail: faizan_ahmad@yahoo.com

U. Das · A. Srinivasan · T. P. Singh
Department of Biophysics,
All India Institute of Medical Sciences,
Ansari Nagar,
New Delhi 110029, India

Introduction

It is well known and widely discussed that there are families of functionally and evolutionary related proteins which have similar overall 3D structures (folding patterns) but quite different amino acid sequences [1, 2]. This does not mean, of course, that protein 3D structures do not depend on the protein sequences. However, it implies that not all features of the protein sequence is important for its folding pattern. The usual explanation of this phenomenon is that the protein-folding pattern is determined not by all details of the amino acid sequences but by the key characteristics of the sequences of all proteins of a given family [3]. That is, just a few identical or conserved residues are enough to ensure the common folding patterns of these proteins. Both experiment and theory have shown that these conserved residues form a folding nucleus which is specific, i.e., it involves a definite set of native contacts, and that the residues which form the nucleus are scattered along the chain [3].

Cytochrome *c*, a 104-residue protein, is a member of an extended family of heme proteins involved in electron transfer functions in the mitochondrial respiratory chain and bacterial photosynthesis [4]. Despite their highly divergent amino acid sequences, these cytochromes *c* share some common structural features, including the covalent linkage of the heme group to two Cys residues, the axial ligands of the heme iron, and a cluster of three α-helices grouped

around one edge of the heme. The total number of conserved residues in the subfamilies of cytochrome *c* considered is surprisingly small. Four conserved residues Cys14, Cys17, His18, and Met80 bind to the heme. Four nonfunctional conserved residues (Gly/Ala6, Phe/Tyr10, Leu/Val/Phe94, Tyr/Trp/Phe97) form, on average, 23 interatomic contacts between N- and C-terminal helices, substantially contributing to the stability [3]. Besides these interhelical contacts, there are a number of contacts inside or near the C-end of the N-terminal helix. This interface involves the conserved residues Leu94 and Tyr97 of the C-terminal helix and Gly6 and Phe10 of the N-terminal helix in cytochrome *c* from horse heart. The side chain of Leu94 packs into the hole created by Gly6 with a peg-in-hole interaction, while Tyr97 and Phe10 pack against each other through an aromatic–aromatic interaction [3]. These sets of conserved nonfunctional residues at the interface between N- and C-terminal helices suggest that these residues are of special importance for the structure and/or the folding of cytochrome *c*. It is assumed that they are involved in a common folding nucleus of all subfamilies of *c*-type cytochromes.

One may exploit the potential offered by site-directed mutagenesis to alter specific interactions in the protein and, consequently, gain insight into the role of such interactions. To determine the importance of noncovalent interactions offered by the side-chain atoms of the conserved Leu94 residue in the stability and folding of native horse cytochrome *c*, we made a novel amino acid substitution of Leu by Gly at position 94. The choice of this mutant was based on our structural analysis using the CCP4 package [5]. In this communication we show that (1) at pH 6.0 and 25 °C the L94G mutant exists as a molten globule (MG) whose midpoint of thermal denaturation is 28 °C less than that of the wild-type protein and (2) at pH 2.0 and 25 °C NaCl induces a cooperative transition between the acid-denatured state (D state) and a state of the mutant having all the common structural characteristics of a pre-MG state.

Materials and methods

Structural analysis

The crystal structure of horse cytochrome *c* [6] was analyzed using 3D structure analysis tools. Leu was mutated to Gly at position 94 by using the Coot package of the CCP4 suite [5]. The structure of the mutant was checked by PROCHEK [7] and Ramachandran plot [8] for its accuracy. The ribbon diagram was drawn using PyMOL [9]. Contacts between Leu94 and other residues in the wild-type protein and those between Gly94 and other residues in the mutant protein were determined using the contact program from the CCP4 package.

Construction of the mutant

The expression plasmid, pBTR containing wild-type horse cytochrome *c* gene and heme lyase, was a kind gift from Professor Gary Pielak, University of North Carolina, USA. This plasmid construct was used for making the mutant L94G protein. The L94G mutation was carried out by site-directed mutagenesis using the PCR-based QuikChange site-directed mutagenesis kit (Stratagene, USA). The following primers (Microsynth, Switzerland) were used:

Primer 1: 5′ GAACGCGAAGACGGCATCGCGTACC TGAAAAAG 3′
Primer 2: 5′ CTTTTTCAGGTACGCGATGCCGTCTT CGCGTTC 3′

Mutation was confirmed by DNA sequencing (Applied Biosystem, USA). A positive clone was used for the mutant protein expression in *Escherichia coli* BL21 (DE3) strain.

Purification of mutated horse cytochrome *c*

Mutated cytochrome *c* protein was purified according to the protocol followed by Patel et al. [10] with a slight modification. Briefly, inoculation (1%) of 1 L of rich medium (12 g bactotryptone, 24 g yeast extract, 4 mL glycerol, 2.3 g KH_2PO_4, 12.5 g K_2HPO_4) was done with overnight primary culture. Ampicillin was added to the culture to a final concentration of 100 μg/L. Cells were grown at 37 °C in a shaker incubator for 36 h at 200 rpm. Cells were harvested and cell paste was resuspended in lysis buffer containing 50 mM tris(hydroxymethyl)aminomethane–Cl, pH 6.8, 1 mM EDTA (3 mL/g cell paste). Cells were sonicated on ice (Bandelin sonicator, Bandelin, Germany) with five pulses of 10 s at an interval of 2 min. The lysate was centrifuged at 8,000 rpm for 20 min and the supernatant was collected. Ammonium sulfate was added to the supernatant to a final concentration of 300 g/L while stirring the mixture on ice, and the mixture was centrifuged at 8,000 rpm for 20 min at 4 °C and the supernatant was collected. This supernatant was dialyzed against distilled water at 4 °C with two changes every 8 h. The dialysate was concentrated on a 3-kDa MWCO Centricon filter (Millipore, USA) to less than 50 mL and dialyzed against low-salt buffer (0.878 g/L NaH_2PO_4, 3.656 g/L Na_2HPO_4). The dialysate was loaded onto a preequilibrated SP-Sepharose cation-exchange column (Sigma, USA). The mutant was eluted with high-salt buffer (0.652 g/L NaH_2PO4, 4.096 g/L Na_2HPO_4, 58.44 g/L NaCl) using a linear gradient. Fractions of 3 mL each were collected and A_{280} and A_{410} (where *A* represents absorbance) were measured. All fractions having an absorbance ratio (A_{410}/A_{280}) greater than 4 were pooled in one tube. Both native and sodium dodecyl sulfate polyacrylamide gel electrophoresis were performed to check the purity.

The final yield of the purified mutant cytochrome *c* (L94G) was found to be 5 mg/L of culture. (The yield of wild-type cytochrome *c* was 15 mg/L.)

Preparation of solutions

Both wild-type and purified L94G cytochrome *c* were oxidized by adding 0.1% potassium ferricyanide as described earlier [11]. The concentration of the oxidized cytochrome *c* was determined experimentally using a value of 106,000 M^{-1} cm^{-1} for the molar absorption coefficient (ε) at 409 nm [12]. A value of 5,000 M^{-1} cm^{-1} for ε at 350 nm was used to determine the concentration of 1-Anilino-8-naphthalene sulfonate (ANS) [13]. The samples were prepared as follows. For the native state (N state), each protein solution was prepared in 0.03 M cacodylate buffer containing 0.1 M NaCl at pH 6.0. The acid-denatured proteins were prepared by incubating them in a water–HCl mixture at pH 2.0. The A state of the wild-type protein was induced by the addition of 1 M NaCl to the acid-denatured protein [11]. The acid-denatured L94G mutant was titrated with NaCl. The titration curve shows that the acid-denatured mutant is transformed to a new state in the presence of an NaCl concentration of 1.0 M or higher, called here the "X state."

Absorbance measurements

Absorption spectra (720–660 nm) of both wild-type horse cytochrome *c* and the L94G mutant were measured using a Shimadzu 1601 UV/vis spectrophotometer at 25.0 ± 0.1 °C. The temperature of the cell compartment was maintained by circulating water from an external thermostated water circulator. The protein concentrations used for the absorption measurements were in the range 75–80 μM. A cell of 1.0-cm path length was used for the absorption measurements.

Circular dichroism measurements

The far-UV circular dichroism (CD) spectra (200–250 nm) were recorded with a JASCO 715 spectropolarimeter using a 1 mm path length cell. For the near-UV CD (270–300 nm) and Soret CD (370–450 nm) measurements, a 1 cm path length cuvette was used. CD spectra of proteins were measured at 25 ± 0.1 °C. Each spectrum was corrected for the blank contribution. The protein concentration used was 18–20 μM. The raw CD data were converted into the mean residue ellipticity $[\theta]_\lambda$, (deg cm^2 $dmol^{-1}$) at wavelength λ using the relation

$$[\theta]_\lambda = M_o\theta_\lambda/10lc$$

where θ_λ is the observed ellipticity in millidegrees at wavelength λ, M_o is the mean residue weight of the protein, *c* is the protein concentration in milligrams per milliliter, and *l* is the path length of the cell in centimeters. The protein-to-ANS molar ratio used for measurements in the far-UV region was 1:20 at pH 6.0.

Fluorescence measurements

Fluorescence spectra were measured using a JASCO FP 6200 spectrofluorimeter (Tokyo, Japan) in a 5-mm quartz cell whose temperature was maintained at 25 ± 0.1 °C by circulating water from an external thermostated water circulator. A slit width of 10 nm was used for excitation and emission. For the Trp fluorescence measurements, the excitation wavelength was 280 nm, and emission spectra were recorded from 300 to 440 nm. For the ANS fluorescence in ANS–protein binding experiments, the excitation wavelength was 360 nm, and emission spectra were recorded from 400 to 600 nm. The protein concentration used for Trp and ANS fluorescence measurements was 7–10 μM. The protein-to-ANS molar ratio for the fluorescence study was 1:20.

Thermal denaturation measurements

Heat-induced denaturation of horse cytochrome *c* and its mutant was carried out in a JASCO spectropolarimeter (model J-715) and a JASCO V-560 UV/vis spectrophotometer equipped with a Peltier-type temperature controller with a heating rate of 1 °C/min, a scan rate providing adequate time for equilibration. Changes in $[\theta]_{222}$ of each protein were measured in the temperature range 20–85 °C. After denaturation, the sample was immediately cooled to measure the reversibility of the process at different temperatures. The data (*y*, *T*) were fitted to a two-state denaturation model using the relation [14, 15]

$$y(T) = \frac{y_N(T) + y_D(T)\exp[-\Delta H_m/R(1/T - 1/T_m)]}{1 + \exp[-\Delta H_m/R(1/T - 1/T_m)]} \quad (1)$$

where $y(T)$ is the experimentally observed optical property of the protein at temperature *T* in kelvins, $y_N(T)$ and $y_D(T)$ are the optical properties of the native (N) and denatured (D) molecules at temperature *T* in kelvins, *R* is the universal gas constant, and ΔH_m is the van't Hoff enthalpy change at T_m, the midpoint of the thermal denaturation. All solution blanks showed negligible changes in measurable parameters with temperature and were, therefore, neglected during the data analysis.

Dynamic light scattering measurements

Dynamic light scattering measurements were carried out using a RiNA Laser Spectroscatter-201 to obtain hydrodynamic radii of different states of cytochrome *c* and L94G

mutant at 25 ± 0.1 °C. Each sample contained 2.5 mg/mL protein. Measurements were made at a fixed angle of 90° using an incident laser beam of 689 nm. Ten measurements were made with an acquisition time of 30 s for each sample at a sensitivity of 10%. The data were analyzed for hydrodynamic radii using PMgr version 3.01 p17, provided by the manufacturer.

Results

Selection and design of the mutant

It is quite evident from the sequence alignment of various cytochromes *c* that, apart from the heme binding residues, there are a few residues which are evolutionarily conserved in these proteins. These are identified as Gly/Ala6, Phe/Tyr10, Leu/Val/Phe94, and Tyr/Trp/Phe97. They are also considered to be involved in the common folding nucleus of all subfamilies of cytochromes *c* [3]. It may be seen from the known coordinates of horse cytochrome *c* that there are a number of interactions within these four residues (Gly6, Phe10, Leu94, and Tyr97), which hold the N- and C-terminal helices of cytochrome *c* [6]. We tried to make a feasible mutant which could help us to determine the importance of these interactions in holding these helices. Gly6 cannot be replaced by any other residues because of their bulkier side chains; hence, they can cause a severe packing defect in the protein structure. Phe10 interacts with Tyr97 of the protein through aromatic–aromatic interaction, which is important for the stability of the protein [3]. In fact, we tried to make mutants to disrupt this aromatic–aromatic interaction by replacing Phe10 with Gly, Val, and Ile, but none of them could be expressed in *E. coli*. The crystal structure of horse cytochrome *c* [6] shows that the side chain of the conserved Leu94 may be important for pairing of the N- and C-terminal helices (Fig. 1) and protein stability, because this residue has interactions with Gly6, Ile9, and Phe10 (Table 1). To try to understand the role of Leu94 in this helix–helix interaction and in the global stability, we mutated this residue of wild-type cytochrome *c* to Gly and characterized the variant. The results of various structural measurements of both the wild type and this mutant are described in the following sections.

Structural characterization of wild-type cytochrome *c* and the L94G mutant by CD measurements

Measurements of the far-UV CD provide information regarding the secondary structure of proteins. Figure 2a shows the far-UV CD spectra of the wild type (curve 1) and the L94G mutant (curve 2) in the native buffer (0.03 M cacodylate, pH 6.0) at 25 °C. This figure also shows the spectrum of the wild-type protein in the presence of 1 M NaCl at pH 2.0 and 25 °C (curve 3). This state of the protein under this experimental condition is customarily called the "A state" [16]. The properties of the A state are similar to the reported properties of the MG state [17]. The L94G mutant was denatured at pH 2.0 and titrated with NaCl (Fig. 2a, inset). It is seen in the inset that this neutral salt induces a transition which is completed at 1 M NaCl. Curve 4 in Fig. 2a shows the CD spectrum of the mutant in the presence of 1 M NaCl at pH 2.0. This state will be referred to here as the "X state." Curves 5 and 6 in Fig. 2a show the spectra of the D state of the wild-type and mutant proteins, respectively.

The near-UV CD spectra of proteins provide information regarding the status of aromatic side chain packing. In

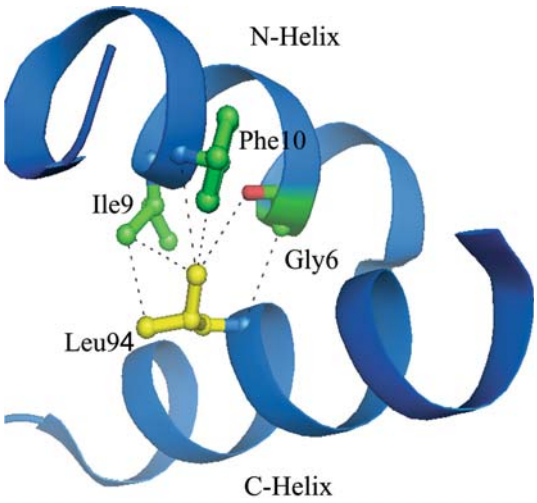

Fig. 1 Model showing the packing of N- and C-terminal helices in horse cytochrome *c*. The pairing of N- and C-terminal helices involves interaction between Gly6, Ile9, Phe10, and Leu94

Table 1 Van der Waals interactions between side chains of Leu94 and other residues

Source atoms		Target atoms	Distance (Å)[a]
94 A LEU C^{β}	…	90 A GLU O	3.47
94 A LEU C^{β}	…	91 A ARG O	3.88
94 A LEU $C^{\delta1}$	…	10 A PHE N	3.86
94 A LEU $C^{\delta1}$	…	6 A GLY O	3.99
94 A LEU $C^{\delta1}$	…	10 A PHE C^{β}	3.74
94 A LEU $C^{\delta1}$	…	10 A PHE C^{α}	3.86
94 A LEU $C^{\delta2}$	…	85 A ILE $C^{\delta1}$	3.25
94 A LEU $C^{\delta2}$	…	68 A LEU $C^{\delta1}$	3.96
94 A LEU $C^{\delta2}$	…	9 A ILE $C^{\gamma2}$	3.94
94 A LEU $C^{\delta2}$	…	105 HEM $C^{\beta\beta}$	3.86

[a] Distance was calculated using the contact program of the CCP4 package [5]

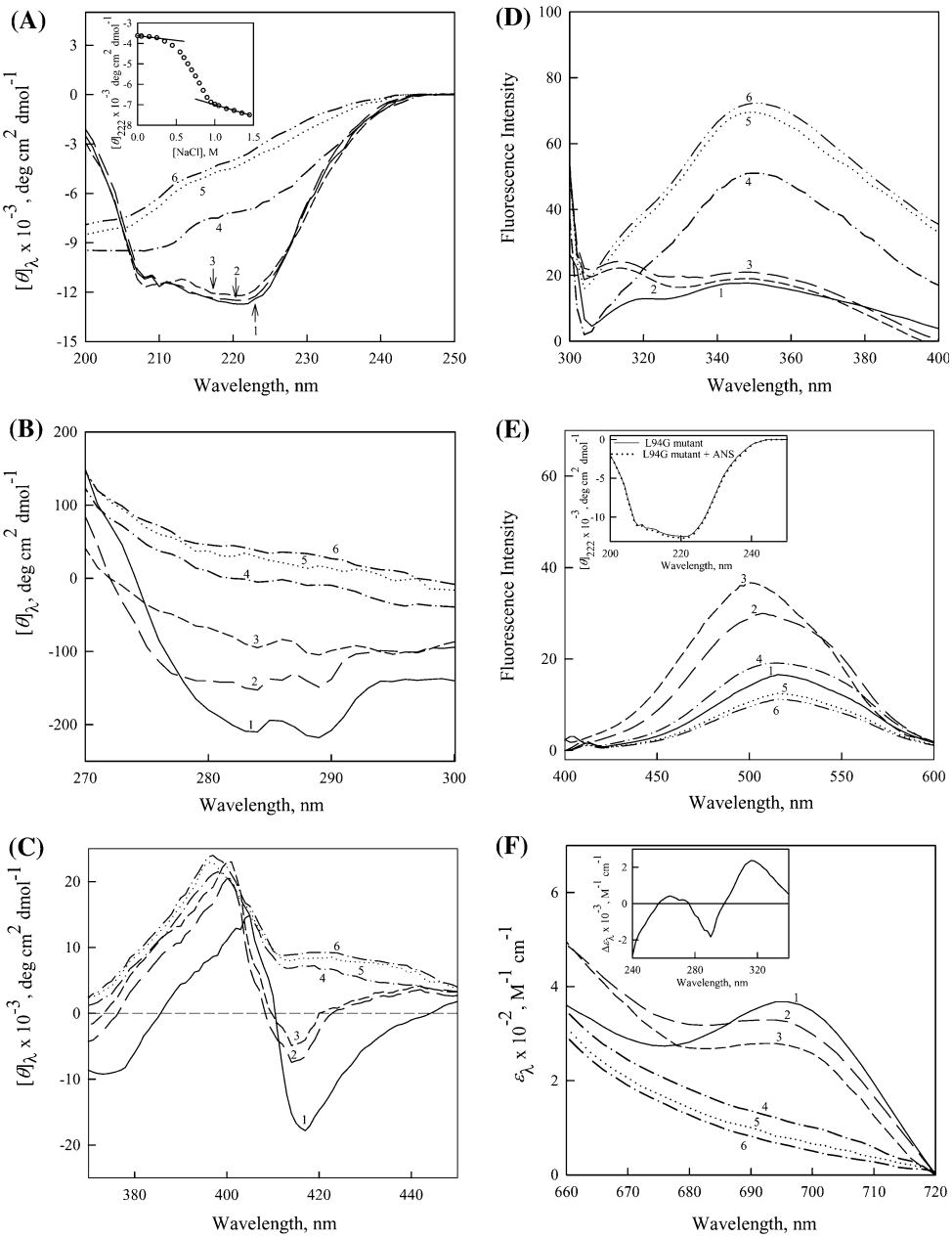

Fig. 2 **a** The far-UV circular dichroism (CD) spectra of wild-type cytochrome *c* in N (curve *1*), A (curve *3*), and D (curve *5*) states and those of the L94G mutant in the native buffer (curve *2*), the X state (curve *4*), and the D state (curve *6*). See the text for an explanation of the states. The *inset* in **a** shows the NaCl-induced transition of the acid-denatured mutant at pH 2.0. **b–f** The near-UV CD, Soret CD, Trp fluorescence, 1-Anilino-8-naphthalene sulfonate (ANS) fluorescence, and absorbance measurements, respectively. The *curve numbers* have the same meaning as in **a**. The *inset* in **e** shows the far-UV CD spectra of L94G in the presence and in absence of ANS at pH 6.0. The *inset* in **e** shows the near-UV difference spectrum of the L94G mutant versus the wild-type protein at pH 6.0. All measurements were carried out at 25 ± 0.1 °C

case of horse cytochrome *c* the characteristic native peaks observed in the region 282–289 nm are attributed to the Tyr side chains [18] and the interaction of Trp59 with the heme propionate [17]. Figure 2b shows the near-UV CD spectra of wild-type horse cytochrome *c* in the N (curve 1), A (curve 3), and D states (curve 5). This figure also shows the near-UV CD spectra of different states of the mutant, the state in the native buffer (curve 2), the X state (curve 4), and the D state (curve 6).

The Soret CD spectrum of native cytochrome *c* in the range 360–450 nm is due to the Phe82 and Met80 axial bond [19]. Figure 2c shows the Soret CD spectra of both wild-type and mutant proteins in different solvent conditions. Curves 1, 3, and 5 represent the spectra of the wild-type protein in the N, A, and D states, respectively. Curves 2, 4, and 6 represent spectra of the mutant L94G in the native buffer, the X state and the D state, respectively.

Fluorescence measurements

Horse cytochrome *c* has a single Trp residue at position 59, which is at a distance of 1 Å from the heme [20]. In the wild-type protein, the fluorescence of Trp is quenched owing to resonance energy transfer to the adjacent heme groups attached to Cys residues at positions 14 and 17 [17]. Figure 2d shows the fluorescence spectra of the wild-type

protein in the N (curve 1), A (curve 3), and D (curve 5) states. This figure also shows the spectra of the L94G mutant in the native buffer (curve 2), the X state (curve 4), and the D state (curve 6).

The presence of exposed hydrophobic clusters and their binding with hydrophobic dyes such as ANS is one of the properties of the MG state [21]. Figure 2e shows ANS fluorescence spectra in the presence of the wild-type protein in the N (curve 1), A (curve 3), and D (curve 5) states. This figure also shows the ANS fluorescence spectra in the presence of the mutant L94G in the native buffer (curve 2), the X state (curve 4), and the D state (curve 6).

Absorbance measurements

Figure 2f shows the absorption spectra (660–720 nm) of the wild-type and mutant proteins. A positive peak at 695 nm in the native wild-type cytochrome *c* spectrum is diagnostic for the presence of a Met80–Fe(III) axial bond [22]. Curves 1, 3, and 5 in Fig. 2f represent spectra of the wild-type protein in its N, A, and D states, respectively. Spectra of the L94G mutant in the native buffer (curve 2), the X state (curve 4), and the D state (curve 6) are also shown in this figure.

Dynamic light scattering measurements

To determine the hydrodynamic radius (R_h) of the protein under different solvent conditions, dynamic light scattering measurements were performed at 25 °C. It has been observed that R_h values of native wild-type cytochrome *c* and the L94G mutant in native buffer are 1.54 ± 0.02 and 1.71 ± 0.04 nm, respectively. The hydrodynamic radii of the wild-type protein in the A and D states are 1.82 ± 0.09 and 3.61 ± 0.05 nm, respectively. Values of 2.2 ± 0.13 and 3.63 ± 0.08 nm for the hydrodynamic radii of the X and D states, respectively, of the L94G mutant were observed.

Thermal stability of mutant cytochrome *c*

To try to understand the role of the mutated amino acid residue in the thermal stability of the protein, heat-induced denaturation curves of the mutant (L94G) and wild-type cytochromes *c* in the native buffer were measured by monitoring changes in absorbance at 405 nm ($\Delta\varepsilon_{405}$) and CD at 222 nm ($[\theta]_{222}$) in the temperature range 20–85 °C (Fig. 3). It has been observed that the thermal denaturation of both the wild-type and the mutant protein is reversible. The data (y, T) were fitted to a two-state denaturation model using Eq. 1 for the estimation of T_m and ΔH_m. The values of T_m and ΔH_m for the wild-type protein (Table 2) are in excellent agreement with those reported earlier [23]. Table 2 also shows T_m and ΔH_m values for the L94G mutant in the native buffer. It is seen in this table that both the T_m and the ΔH_m values for a protein obtained by two different optical probes are, within experimental error, identical. This agreement led us to conclude that the heat-induced denaturation of the mutant and wild-type proteins is a two-state process. Indeed, it has been reported that heat induces a two-state denaturation of horse cytochrome *c* [23]. Assuming that the wild-type and mutant proteins have a ΔC_p value of 1.30 kcal mol^{-1} K^{-1} [24], we estimated ΔG°_D, the Gibbs energy change at 25 °C, using the Gibbs–Helmholtz equation,

$$\Delta G^{\circ}_D = [\Delta H_m(T_m - 298.15)/T_m] - \Delta C_p[(T_m - 298.15) + 298.15\ln(298.15/T_m)]$$

with values of T_m and ΔH_m given in Table 2. The values of ΔG°_D thus estimated are given in Table 2. Identical values for this thermodynamic parameter of a protein obtained by two different optical methods suggest that the heat-induced denaturation of the mutant as well as that of wild-type protein is a two-state process.

Discussion

The analysis of the known 3D structure of wild-type horse cytochrome *c* reveals that there are ten van der Waals interactions between the side-chain atoms of Leu94 and atoms of Gly6, Ile9, Phe10, Leu68, Ile85, Gln90, Arg91, and heme that occur between N- and C-terminal helices (Table 1). Figure 1 shows six of these interactions. All the ten van der Waals interactions will vanish on the substitution of Gly for Leu at position 94. It is therefore expected that the L94G mutant will be less stable than the wild-type protein. To estimate the extent of destabilization, we measured the stability of both wild-type and mutant proteins (Fig. 3). The analysis of thermal denaturation curves for T_m reveals that the L94G mutant has a T_m value which is 28 °C less than that of the wild-type protein (Table 2). This analysis also gave values for ΔH_m, the enthalpy change at T_m (Table 2). It is seen in Table 2 that the ΔH_m value for the wild-type protein is significantly more than that for the L94G mutant, which is devoid of at least ten van der Waals interactions. That the mutant is significantly destabilized is also evident from our ΔG°_D measurements (Table 2). Although it is difficult to quantitate the van der Waals contribution to the protein stability, the average energy per atom pair is 0.15 kcal mol^{-1} at 25 °C [25]. It is then obvious that the L94G mutant will be at least 1.5 kcal mol^{-1} less stable than the wild-type protein. However, Table 2 shows that the mutant is destabilized by about 5 kcal mol^{-1}. This suggests that other stabilizing interactions are also absent in the mutant protein. The reason for saying this is that there are many noncovalent

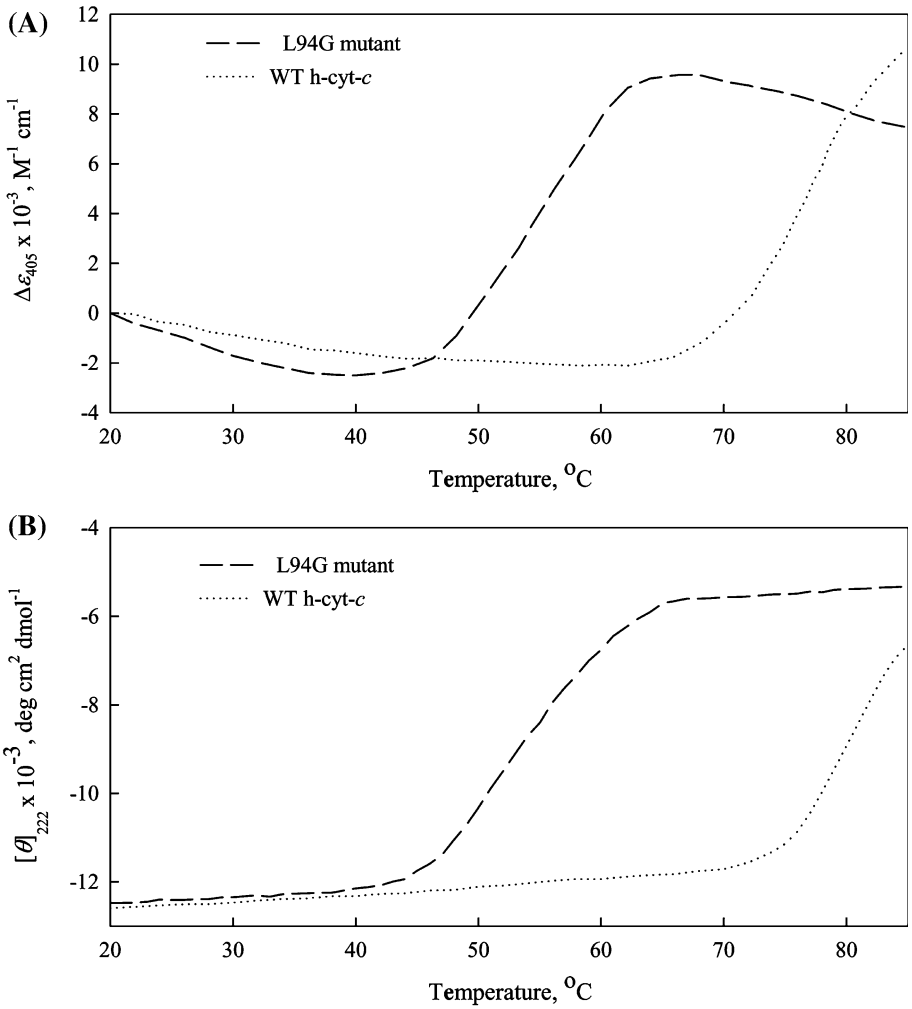

Fig. 3 Thermal denaturation of wild-type horse cytochrome *c* and its L94G mutant monitored by $[\theta]_{222}$ (**a**) and $\Delta\varepsilon_{405}$ (**b**) at pH 6.0. *WT h-cyt-c* wild-type horse cytochrome *c*

Table 2 Thermal denaturation of proteins in the native buffer

Probe	Wild-type horse cytochrome *c*			L94G mutant		
	T_m (°C)	ΔH_m (kcal mol^{-1})	ΔG^o_D (kcal mol^{-1})	T_m (°C)	ΔH_m (kcal mol^{-1})	ΔG^o_D (kcal mol^{-1})
$[\theta]_{222}$	83.1 ± 0.3	101 ± 5	9.9 ± 0.6	54.7 ± 0.4	76 ± 3	5.06 ± 0.13
$\Delta\varepsilon_{405}$	82.8 ± 0.2	99 ± 4	9.6 ± 0.3	54.2 ± 0.3	75 ± 3	4.96 ± 0.2

The ± sign represents the deviation from the mean value of triplicate measurements

interactions, including 36 of them between heme and amino acid residues, that stabilize the wild-type protein [6]. In the absence of the 3D structure of the L94G mutant, it is, however, not possible to say which noncovalent interactions other than those shown in Table 1 are perturbed on the mutation of Leu94.

Although the L94G mutant is thermodynamically less stable than the wild-type protein (Table 2), the far-UV CD measurements revealed that the overall secondary structures present in both proteins are almost identical (Fig. 2a, curves 1 and 2). This suggests that stabilizing noncovalent interactions, including van der Waals interactions holding the N- and C-terminal helices (Fig. 1), are not important for guiding the formation of the secondary structure of cytochrome *c*.

Leu94, Phe10, and Gly6 are considered to be involved in a common folding nucleus which guides the protein to fold properly [3]. The mutation of Leu to Gly at position 94 may lead to improper folding at the level of the tertiary structure. To check this, we determined the tertiary structure of the L94G mutant and compared it with that of the wild-type protein. A comparison of the near-UV CD spectrum of wild-type horse cytochrome *c* (Fig. 2b, curve 1) with that of the L94G mutant in the native buffer

(Fig. 2b, curve 2) shows that there is a considerable loss of aromatic CD of the mutant. This weak CD signal observed in the mutant may be due to improper packing of Tyr side chains and/or decrease in heme–Trp interaction [17, 18]. Since the Trp fluorescence spectra of the mutant and wild-type proteins are very similar, it seems that the heme–Trp distance is largely maintained in L94G (Fig. 2d, curves 1 and 2). To show that the reduction in CD of the mutant (Fig. 2b, curve 2) is due to the exposure of the aromatic amino acid residues to the polar solvent and not due to reduction in their asymmetry only, we measured the difference absorption spectrum of the mutant against the wild-type protein. It is seen in the inset of Fig. 2f that the L94G mutant has its aromatic residues exposed to the polar water solvent [26], because a decrease in $\Delta\varepsilon_{287}$ is also a signature of exposure of Tyr from a nonpolar to a polar solvent. Thus, the mutant in the native buffer has less tertiary structure than the wild-type protein.

The common structural characteristics of the MG state are as follows: (1) the presence of a pronounced amount of secondary structure, (2) the absence of most of the specific tertiary structure produced by the tight packing of side chains, (3) the compactness of the protein molecule with a radius of gyration 10–30% larger than that of the native state, and (4) the presence of a loosely packed hydrophobic core that increases the hydrophobic surface accessible to the solvent [21]. A comparison of the far- and near-UV CD spectra of native wild-type horse cytochrome *c* (Fig. 2a, b, curves 1) with those of the L94G mutant in the native buffer (Fig. 2a, b, curves 2) suggests that the mutant has two of the structural characteristics of the MG state, namely, characteristics 1 and 2 mentioned above. However, comparison of the near-UV CD spectrum of the L94G mutant in the native buffer (Fig. 2b, curve 2) with that of its D state (Fig. 2b, curve 6) suggests that the characteristic native tertiary interactions in the wild-type protein (Fig. 2b, curve 1) are only partially lost in the mutation-induced MG state. This finding is consistent with the reports that there is remarkable diversity among MG states of a protein induced by different solvent conditions [21, 27], and there is substantial nativelike tertiary packing in the MG states of some proteins [21].

To ascertain whether the L94G mutant has other MG-like characteristics, we carried out fluorescence measurement of ANS in the presence of wild-type and mutant proteins under different solvent conditions (Fig. 2e), because the dye shows increase in fluorescence intensity with a blueshift in the emission maximum on binding with exposed hydrophobic clusters known as finger prints of the MG state [28]. Our observations suggest that there is blueshift in the emission maximum of the dye in the presence of the mutant and an increase in fluorescence intensity. This observation suggests that the L94G mutant has more hydrophobic patches exposed to the polar solvent than the wild-type protein. It was shown earlier that ANS induces a secondary structure in acid-denatured wild-type cytochrome *c* at pH 2 [29]. To see whether the dye induces a secondary structure, we measured the far-UV CD of the L94G mutant in the presence and absence of ANS. It was observed that ANS does not alter the secondary structure content of the L94G mutant at pH 6.0 (Fig. 2e, inset).

To further characterize the state of the the L94G mutant in the native buffer, we measured its hydrodynamic radius (R_h) and compared it with the observed R_h of wild-type horse cytochrome *c*. For a solid sphere, R_h is related to R_G through the relation $R_G^2 = 3R_h^2/5$ (Eqs. 18–20 in [30]. We estimated R_G values from the observed values of R_h of the wild type and the mutant in the native buffer. It was found that the compactness of the L94G mutant is 14% larger than that of the wild-type protein, which qualifies the mutant to have characteristic 3 mentioned above. These measurements and the optical characterizations of the L94G mutant in the native buffer and their comparison with those of wild-type cytochrome *c* (Fig. 2) led us to conclude that a single mutation in wild-type horse cytochrome *c* induces a MG state.

Various MG-like thermodynamically stable intermediates have been observed in wild-type horse cytochrome *c*, and only MG states induced by NaCl (pH 2.0) and weak salt denaturants (LiCl, $CaCl_2$, $LiClO_4$) are well characterized in terms of thermodynamic [23, 27, 31] and structural [17, 32] parameters at pH 6.0. Table 3 compares these parameters of the MG state of the L94G mutant only with those of the wild-type protein induced by $LiClO_4$ and LiCl at pH 6.0 at 25 °C and NaCl (pH 2.0) at 25 °C because $CaCl_2$- and LiCl-induced MG states have been shown to have identical structural and thermodynamic properties [27]. Since a comparison of the A state with various MG states of wild-type horse cytochrome *c* induced by LiCl and $LiClO_4$ has already been presented and discussed in detail elsewhere [33], we shall not repeat it here. Instead, we shall present a comparison of structural and thermodynamic characteristics of the mutation-induced MG state with those of the A state of the wild-type protein. The helical content of both MG states are, within experimental error, identical (Fig. 2a, curves 1 and 2). This finding is consistent with the argument that the hydrophobic core composed of main helix segments of wild-type protein is retained in the acid-induced MG state [20, 33, 34]. It is seen in Fig. 2 that the L94G mutant (curves 2) retains more tight packing of aromatic side chains (Fig. 2b), heme–globin interaction (Fig. 2c), hydrophobic surface area (Fig. 2e), and Met80–Fe(III) interactions (Fig. 2f) compared with the A state (Fig. 2b–f, curves 3). If this is the case, it is then expected that the L94G mutant is not only structurally different from other MG states of wild-type

Table 3 A comparisons of structural properties of the L94G mutant in the native buffer (pH 6.0) with those of various molten globule states of wild-type horse cytochrome *c* at 25 °C

Property	L94G mutant	Wild-type horse cytochrome *c*		
	pH 6.0	Acid	LiCl[a]	$LiClO_4$[a]
$[\theta]_{222}$ (deg cm^2 $dmol^{-1}$)	−12,700	−11,900	−12,200	−11,100
$[\theta]_{287}$ (deg cm^2 $dmol^{-1}$)	−115	−90	−85	−7
$[\theta]_{416}$ (deg cm^2 $dmol^{-1}$)	−6,900	−4,500	−4,500	−6,700
ε_{695} (M^{-1} cm^{-1})	327	266.4	69.8	79
Trp fluorescence intensity at λ_{max}	19	14.6	14.2	34.9
ANS fluorescence intensity at λ_{max}	29	35	29.2	25.2
R_G (Å)	14	15	15	17
$\Delta G_{MG\leftrightarrow D}$ (kcal mol^{-1})	5	2.8[a]	1.5	1.3

ANS 1-Anilino-8-naphthalene sulfonate

[a] Taken from Table 2 in [33] except the values of ε_{695}

horse cytochrome *c*, but will also be more stable than the A state, i.e., $\Delta G_{MG\leftrightarrow D}$, ΔG associated with the transition between MG and D states, will be more. This is what was observed here (Table 2).

Wild-type horse cytochrome *c* is denatured at pH 2.0 (Fig. 2a–e, curves 5); however, this acid-denatured protein in the presence of 1 M NaCl undergoes a transition between D and A states [11]. Figure 2 shows spectra of D (curves 5) and A (curves 3) states of wild-type cytochrome *c*. The L94G mutant is also denatured at pH 2.0, and its optical spectra (Fig. 2a–e, curves 6) are almost identical to those of the D state of the wild-type protein (Fig. 2a–e, curves 5). The acid-denatured L94G mutant was titrated with NaCl, and it was observed that NaCl induces a cooperative transition between the thermodynamically stable states D and X (Fig. 2a, inset). It is seen in Fig. 2 (curves 4) that this thermodynamically stable X state has less secondary structure (Fig. 2a), aromatic tertiary structure (Fig. 2b), and globin–heme interaction (Fig. 2c) than the A state, the acid-induced MG state (Fig. 2, curves 3). Furthermore, measurements of Trp fluorescence (Fig. 2d), ANS binding (Fig. 2e), and Met80–Fe(III) interaction (Fig. 2f) present in the X state suggest that these properties are like those of the D state.

A systematic investigation of acid-induced denaturation has shown that wild-type horse cytochrome *c* at low pH acquires a state that is intermediate between the MG and unfolded (D) states [35]. This thermodynamically stable state was called the "pre-MG state" of the protein. The mechanism of formation of this state is the same as that of the MG state [36]. Uversky [36] observed that the pre-MG state has five common structural characteristics: (1) the presence of about 50% of the native secondary structure, (2) the absence of a rigid tertiary structure, (3) the compactness (in terms of hydrodynamic volume) is approximately 3 times that of the N state of wild-type horse cytochrome *c*, (4) the accessibility of the buried Trp is intermediate between MG and D states, and (5) the ANS binding is approximately 5 times weaker than for the MG state. As mentioned in the preceding paragraph, the X state of the L94G mutant has all structural characteristics between those of its MG and D states. We, therefore, asked a question: is the X state of the L94G mutant a pre-MG state? To answer this question we determined the five structural characteristics of the X state mentioned above and compared them with those of wild-type cytochrome *c* and those of the MG and D states of L94G (Table 4). Determination of $[\theta]_{222}$ values

Table 4 A comparison of structural properties of the L94G mutant with those of native wild-type horse cytochrome *c* at 25 °C

Property	Wild-type horse cytochrome *c*[a]	L94G mutant		
		MG[a]	X[b]	D[c]
$[\theta]_{222}$ (deg cm^2 $dmol^{-1}$)	−12,900	−12,700	−6,700	−3,500
$[\theta]_{287}$ (deg cm^2 $dmol^{-1}$)	−205	−115	−3	35
$[\theta]_{416}$ (deg cm^2 $dmol^{-1}$)	−16,000	−6,900	7,100	9,000
ε_{695} (M^{-1} cm^{-1})	367	327	113	62
Trp fluorescence intensity at λ_{max}	18	19	51	72
Relative ANS fluorescence intensity at λ_{max}	0	12	2	−6
Hydrodynamic volume ($Å^3$)	15,304	21,000	44,721	200,895

[a] In the presence of 0.03 M cacodylate buffer containing 0.1 M NaCl at pH 6.0

[b] The X state of L94G was prepared by incubating the protein in a water–HCl mixture in the presence of 1 M NaCl at pH 2.0

[c] The acid-denatured state of the mutant was prepared by incubating the protein in a water–HCl mixture at pH 2.0

(which are a measure of secondary structure) of native wild-type cytochrome *c* and the MG, X, and D states of the L94G mutant suggests that the X state contains about 52% of the secondary structure present in the wild-type protein. Thus, the first criterion of a pre-MG state is fulfilled. Measurements of $[\theta]_{287}$, $[\theta]_{416}$, ε_{695}, ANS binding, and Trp fluorescence of native wild-type horse cytochrome *c* and L94G under different solvent conditions suggest the presence of almost no rigid tertiary structure in the X state of L94G (Table 4). This fulfills the second structural characteristics of a pre-MG state. The third structural characteristic of a pre-MG state is that its hydrodynamic volume is approximately 3 times more than that of the N state of the wild-type protein. Our results given in Table 4 do suggest that the hydrodynamic volume of the X state of L94G is approximately 3 times more than that of wild-type horse cytochrome *c*. Fluorescence measurements suggest that the ANS binding with the X state is 6 times weaker than that with the MG state of the mutant (Table 4). Thus, the structural characteristics of the X state of L94G and their comparison with those of other states led us to conclude that the L94G mutant in the presence of 1 M NaCl at pH 2.0 exits as a pre-MG state.

It is seen in the inset of Fig. 1 that the thermodynamic equilibrium between D and X states is cooperative, suggesting that there exits a specific binding site(s) on the protein in the X state [37]. Assuming a specific binding model, we analyzed this equilibrium for the value of *n*, the number of Cl^- ions bound to the X state, using appropriate relations (see Eqs. 1–3 in [37]). We obtained a value of 1.1 for *n*, suggesting that the X state has one binding site for the Cl^- ion. Thus, the pre-MG (X) state of cytochrome *c* is stabilized by Cl^- binding, although some contributions from general salt effects (Debye–Huckle screening) cannot be ruled out. It is noteworthy that from their kinetic studies, Colon and Roder [37] showed the presence of a kinetic intermediate (I'_C) in the D → MG transition of horse cytochrome *c* at pH 2.0. A comparison of I'_C with the thermodynamically stable pre-MG state observed in this study shows that both have similar properties.

In summary, the native MG state of the L94G mutant is different from the MG states of horse cytochrome *c* [33]. L94G in the presence of 1 M NaCl or more at pH 2.0 exists as a thermodynamically stable pre-MG state.

Acknowledgments This work supported by grants from the CSIR and DST to F.A. M.K.A.K., M.H.R., and M.I.H are thankful to the CSIR, UGC, and DST, respectively, for fellowships.

References

1. Bashford D, Chothia C, Lesk AM (1987) J Mol Biol 196:199–216
2. Chothia C, Lesk AM (1986) EMBO J 5:823–826
3. Ptitsyn OB (1998) J Mol Biol 278:655–666
4. Meyer TE, Kamen MD (1982) Adv Protein Chem 35:105–212
5. Emsley P, Cowtan K (2004) Acta Crystallogr D Biol Crystallogr 60:2126–2132
6. Bushnell GW, Louie GV, Brayer GD (1990) J Mol Biol 214:585–595
7. Laskowski RA, Moss DS, Thornton JM (1993) J Mol Biol 231:1049–1067
8. Ramachandran GN, Sasisekharan V (1968) Adv Protein Chem 23:283–438
9. DeLano WL (2002) The PyMOL molecular graphics system. DeLano Scientific, San Carlos
10. Patel CN, Lind MC, Pielak GJ (2001) Characterization of horse cytochrome *c* expressed in Escherichia coli. Protein Expr Purif 22:220–224
11. Goto Y, Takahashi N, Fink AL (1990) Biochemistry 29:3480–3488
12. Margoliash E, Frohwirt N (1959) Biochem J 71:570–572
13. Mulqueen PM, Kronman MJ (1982) Arch Biochem Biophys 215:28–39
14. Sinha A, Yadav S, Ahmad R, Ahmad F (2000) Biochem J 345(3):711–717
15. Santoro MM, Bolen DW (1988) Biochemistry 27:8063–8068
16. Goto Y, Calciano LJ, Fink AL (1990) Proc Natl Acad Sci USA 87:573–577
17. Santucci R, Bongiovanni C, Mei G, Ferri T, Polizio F, Desideri A (2000) Biochemistry 39:12632–12638
18. Hamada D, Kuroda Y, Kataoka M, Aimoto S, Yoshimura T, Goto Y (1996) J Mol Biol 256:172–186
19. Santucci R, Ascoli F (1997) J Inorg Biochem 68:211–214
20. Dill KA, Chan HS (1997) Nat Struct Biol 4:10–19
21. Arai M, Kuwajima K (2000) Adv Protein Chem 53:209–282
22. Schejter E, Saludjian P (1967) Biopolymers 5:788–790
23. Moza B, Qureshi SH, Ahmad F (2003) Biochim Biophys Acta 1646:49–56
24. Makhatadze GI, Clore GM, Gronenborn AM (1995) Nat Struct Biol 2:852–855
25. Fersht AR (1997) Curr Opin Struct Biol 7:3–9
26. Donovan JW (1973) Methods Enzymol 27:497–525
27. Qureshi SH, Moza B, Yadav S, Ahmad F (2003) Biochemistry 42:1684–1695
28. Semisotnov GV, Rodionova NA, Razgulyaev OI, Uversky VN, Gripas AF, Gilmanshin RI (1991) Biopolymers 31:119–128
29. Ali V, Prakash K, Kulkarni S, Ahmad A, Madhusudan KP, Bhakuni V (1999) Biochemistry 38:13635–13642
30. Tanford C (1961) Physical chemistry of macromolecules. Wiley, New York
31. Kuroda Y, Kidokoro S, Wada A (1992) J Mol Biol 223:1139–1153
32. Jeng MF, Englander SW (1991) J Mol Biol 221:1045–1061
33. Moza B, Qureshi SH, Islam A, Singh R, Anjum F et al (2006) Biochemistry 45:4695–4702
34. Marmorino JL, Pielak GJ (1995) Biochemistry 34:3140–3143
35. Fink AL, Calciano LJ, Goto Y, Kurotsu T, Palleros DR (1994) Biochemistry 33:12504–12511
36. Uversky VN (1997) Protein Pept Lett 4:355–367
37. Colon W, Roder H (1995) Nat Struct Biol 3:1019–1025